HOSTED BY

ELSEVIER
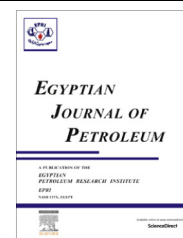
Egyptian Petroleum Research Institute

Egyptian Journal of Petroleum

www.elsevier.com/locate/egyjp
www.sciencedirect.com

EGYPTIAN JOURNAL OF PETROLEUM

FULL LENGTH ARTICLE

Novel naphthenate surfactants based on petroleum acids and nitrogenous bases as corrosion inhibitors for C1018-type mild steel in CO₂-saturated brine

CrossMark

Hany M. Abd El-Lateef [a],*, V.M. Abbasov [b], L.I. Aliyeva [b], Mai M. Khalaf [a]

[a] *Chemistry Department, Faculty of Science, Sohag University, 82524 Sohag, Egypt*
[b] *Mamedaliev Institute of Petrochemical Processes, National Academy of Sciences of Azerbaijan, AZ1025 Baku, Azerbaijan*

Abstract   The efficiency of two natural naphthenate surfactants (Naphthenic-dimethylamine and Naphthenic-diethylamine complexes), as corrosion inhibitors for mild steel in CO₂-saturated 1% NaCl solution, has been determined by linear polarization resistance corrosion rate and potentiodynamic polarization measurements. These compounds inhibit corrosion even at very low concentrations (25 ppm), and Naphthenic-diethylamine complex is the best inhibitor giving maximum inhibition efficiency (99.76) at 100 ppm. Polarization curves indicate that, the two investigated compounds are mixed inhibitors, affecting both cathodic and anodic corrosion currents. Adsorption of naphthenate surfactants on the mild steel surface is in good agreement with the Langmuir adsorption isotherm model, and the calculated Gibbs free energy values confirm the chemical nature of the adsorption. Energy dispersive X-ray fluorescence microscopy (EDRF) and scanning electron microscope (SEM) observations confirmed the existence of such an adsorbed film on the mild steel surface.
© 2015 The Authors. Production and hosting by Elsevier B.V. on behalf of Egyptian Petroleum Research Institute. This is an open access article under the CC BY-NC-ND license (http://creativecommons.org/licenses/by-nc-nd/4.0/).

1. Introduction

Carbon dioxide (CO₂) corrosion of carbon steel pipelines and equipment in the oil and gas industry has been given much attention in recent years because of an increased tendency to inject CO₂ into oil wells to reduce the viscosity of oil and increase its production [1,2]. An important fact is that when

CO₂ dissolves in water, carbonic acid (H₂CO₃) is produced with the characteristic that is more aggressive than hydrochloric acid at the same pH [3]. Despite the fact that carbon steel has low resistance to CO₂ environments, it is widely used in the petroleum industry mainly due to economical reasons [2]. What makes feasible the use of carbon steels is the natural precipitation of protective iron carbonate (FeCO₃) [4,5]. In order to reduce the corrosion of mild steel an alternative is to use inhibitor. The corrosion control by inhibitors is one of the most common, effective and economic methods to protect metals [6,7]. Corrosion inhibition of carbon steel is a result of a barrier film forming between the carbon steel and the environment.

* Corresponding author.
E-mail address: Hany_shubra@yahoo.co.uk (H.M. Abd El-Lateef).

Surfactants are molecules composed of a polar hydrophilic group, the 'head', attached to a non polar hydrophobic group, the 'tail'. In general, in aqueous solution the inhibitory action of surfactant molecules may also be due to physical (electrostatic) adsorption or chemisorption onto the metallic surface, depending on the charge of the solid surface and the free energy change of transferring a hydrocarbon chain from water to the solid surface. The adsorption of the surfactants markedly changes the corrosion resisting property of a metal, and for this reason, studies on the relation between adsorption and corrosion inhibition are of considerable importance [8–11]. The adsorption behavior of surfactants at the solid-solution interface is described by many authors [12,13]. The ability of a surfactant molecule to adsorb is generally related to its ability to aggregate to form micelles. Surfactants have been used for the corrosion inhibition of carbon steel in CO_2 environments [14–17].

The present study aimed to investigate the efficiency of some surfactants as corrosion inhibitors for mild steel in CO_2-saturated 1% NaCl solution. An attempt was also made to clarify the effects of concentration of the studied surfactants on the inhibition efficiency. The measurements of corrosion rate and percentage inhibition efficiency of different natural naphthenates surfactants toward corrosion of mild steel by linear polarization resistance corrosion rate and electrochemical polarization technique were performed in CO_2-saturated solution in the absence and presence of the investigated surfactants in the concentration range (25–100 ppm). Energy dispersive X-ray fluorescence (EDRF) was performed to verify the presence of the inhibitor on the carbon steel surface.

2. Experimental work

2.1. Chemical composition of mild steel alloy

The rotating disk working electrodes for tests were made of mild steel grade C1018 and have an area of 4.55 cm^2 with a chemical composition (wt%) C 0.18%, Si 0.17%, Mn 0.70%, P 0.011%, S 0.03%, Ni 0.0%, Cr 0.01% and Fe balance.

2.2. Synthesis of surfactant inhibitors

The surfactants used as inhibitors were synthesized in our laboratory based on petroleum acids and nitrogenous bases. The new series of the naphthenates surfactants were synthesized from naphthenic acids isolated from light oil fractions (Tb = 180–350 °C) [18]. Naphthenic acids were taken at molar ratio 1:1 with dimethylamine and diethylamine. The components of reactions were mixed well for a period of 30 min at 25 °C. Two complex surfactants were synthesized in high purity by the compositions as shown in Table 1. The chemical structure of the synthesized surfactants was characterized by using FT-IR, Spectrum BX spectrometer using KBr disks.

2.3. Preparation of solutions

The aggressive solutions were made of AR grade 1% NaCl solutions saturated with carbon dioxide gas in 1% NaCl solution which was prepared by dissolving of analytical grade NaCl in distilled water. The concentration range of the

Table 1 List of the synthesized complex surfactants includes, code number, name and structure.

Code number of the inhibitor	Name and abbreviation	Structure
I	Naphthenic-dimethylamine complex (NDMC)	$R\text{-}COO]^{+}NH_2\big\langle{}^{CH_3}_{CH_3}$
II	Naphthenic-diethylamine complex (NDEC)	$R\text{-}COO]^{+}NH_2\big\langle{}^{CH_2\text{-}CH_3}_{CH_2\text{-}CH_3}$

prepared surfactants was from 25 to 100 ppm used for corrosion measurements. All inhibitors solutions were prepared using distilled water.

2.4. Corrosion measurements

The measurements were performed on the rotating cylinder electrode (A = 4.55 cm^2). This electrode was used for one time. The reference electrode was Ag/AgCl electrode to which all potentials are referred.

Before beginning the experiment, the prepared 1% NaCl solution was stirred by a magnetic stirrer for 30 min in 1000 ml cell. Then this cell was thermostated at 50 °C for 1 h under a pressure of 0.9 bars. The solution was saturated with carbon dioxide. To remove any surface contamination and air formed oxide, the working electrode was kept at −1500 mV (Ag/AgCl) for 5 min in the tested solution, disconnected shaken free of adsorbed hydrogen bubbles and then cathodic and anodic polarization was recorded. ACM Gill AC instrument connected with a personal computer was used for the measurements.

The corrosion resistance of the investigated mild steel in 1% NaCl saturated with CO_2 was examined using two different techniques:

2.4.1. Potentiodynamic measurements
The potentiodynamic polarization curves were performed in a potential range ± 100 mV with respect to corrosion potential (E_{corr}) at temperature (50 °C). Three electrodes consisting of a reference electrode (Ag/AgCl), a working electrode (Mild steel) and a counter electrode (Pt electrode) at scan rate of 1 mV/s were used.

2.4.2. Linear polarization resistance corrosion rate
The linear polarization resistance (LPR) corrosion rate bubble-test method involves evaluating the corrosion of steel in simulated brine saturated with CO_2 at a temperature equivalent to that in the field. The LPR method is ideal for plant monitoring offering an almost instantaneous indication of corrosion rate, allowing for quick evaluation of remedial action and minimizing unscheduled downtime. The potential of the working electrode was varied by a CoreRunning programme (Version 5.1.3.) through an ACM instrument Gill AC. The CoreRunning programme converts a corrosion current in mA/cm^2 to a corrosion rate in mm/year. A cylindrical carbon steel rod of the composition 080A15 GRADE STEEL was used as a working electrode. Gill AC technology allows to

measure DC and AC signals using standard Sequencer software. A small sweep from typically -10 mV to $+10$ mV is performed at a rate of 10 mV/min (around the rest potential).

Each experiment was performed with freshly prepared solution. Measurements were conducted at 50 °C for the investigated CO_2-saturated 1% NaCl solution. For this purpose, a Magnetic Stirrer with Heater (115 V, 50/60 Hz) was used.

2.5. Surface analysis

In order to observe any changes in surface morphologies of the mild steel samples after testing, the specimens were first immersed in the tested media with and without an inhibitor for 3 days, then cleaned with bi-distilled water and acetone, and dried with cool air. Then the morphology of the tested sample was observed by using HORIBA XGT-7000 – Energy dispersive X-ray fluorescence (EDRF) conducted with scanning electron microscope (SEM) (EDRF-SEM) (JEOL, model 5300).

3. Results and discussions

3.1. Chemical structure of the synthesized natural naphthenate surfactants

The chemical structures for naphthenate surfactants were confirmed by FT-IR. The FT-IR absorption spectra for surfactant **II** showed an absorption band at the 2330 cm^{-1}, indicating that the amine band was disappearing by emerging ammonium ion ($R{-}NH_2^+{-}$). In addition, there was a strong band at 865 cm^{-1}, indicating the presence of CH_2 groups. The strong band at 1725 cm^{-1} indicates the C$=$O group. The increasing C$=$O group frequency due to a link occurring between the acid proton with the amino nitrogen leads to increasing the attraction of electrons from the carbonyl group. The FT-IR absorption spectra confirmed the disappearance of $-$OH band of acid (broad band), this confirmed the transfer of proton of acid to nitrogen atom of amine to form $-NH_2^+-$ group.

3.2. Potentiodynamic polarization curves

In order to study the effect of naphthenate surfactants on the polarization behavior of mild steel, polarization curves for different concentrations of surfactant **II** in CO_2-saturated 1% NaCl solution at scan rate 1 mV/s and at 50 °C were plotted (Fig. 1). Corrosion parameters were calculated on the basis of cathodic and anodic potential vs. current density characteristics in the Tafel potential region [19]. The values of the corrosion current density (I_{corr}) for the mild steel in the absence and presence of investigated surfactants were determined by the extrapolation of the cathodic and anodic Tafel lines to corrosion potential (E_{corr}). The inhibition efficiency is calculated by the following expression:

$$\eta\% = \frac{I_{uninh.} - I_{inh.}}{I_{uninh.}} \times 100 \tag{1}$$

where $I_{uninh.}$ and $I_{inh.}$ are the uninhibited and inhibited corrosion currents. The inhibited corrosion currents are those determined in the presence of the studied surfactants used in this investigation. The uninhibited corrosion currents were determined in pure (inhibitor free) CO_2-saturated 1% NaCl
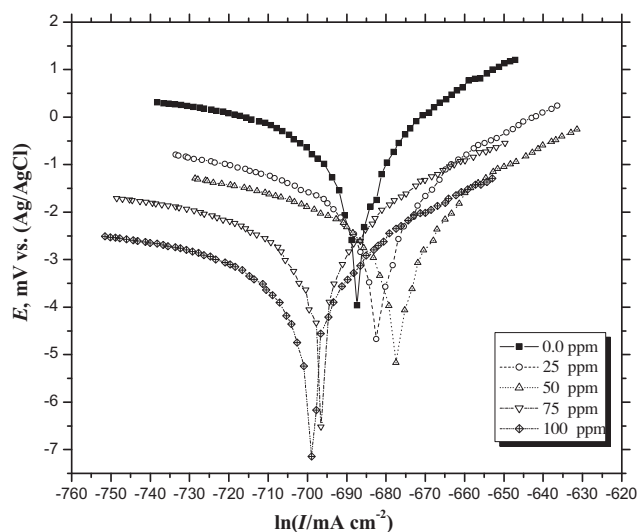

Figure 1 Tafel polarization curves for mild steel in CO_2-saturated 1% NaCl solution containing different concentrations of inhibitor (**II**) at 50 °C.

solution at the same temperature. As can be seen , a marked shift occurs in both cathodic and anodic branches of the polarization curves of mild steel toward lower current densities in the presence of surfactants molecule. This means that, the surfactants affect both cathodic and anodic reactions. It was found that, both anodic and cathodic reactions of mild steel electrode corrosion were inhibited with increasing concentration of synthesized inhibitors. These results suggest that not only the addition of synthesized inhibitors reduce anodic dissolution but also retard the hydrogen evolution reaction. A similar behavior was observed after the addition of inhibitor **I** to the CO_2-saturated brine. It is also obvious that inhibitor **II** has a higher inhibition efficiency than inhibitor **I** at all investigated concentrations.

The values of I_{corr}, cathodic (β_c) and anodic Tafel (β_a) slopes were obtained by fitting the polarization data in the vicinity of $E_{corr} \pm 100$ mV (The slopes of the cathodic (β_c) and anodic (β_a). Tafel lines were calculated by using CoreRunning programme (Analysis data graph)), E_{corr}, degree of surface coverage (θ) and the inhibition efficiency ($\eta\%$) obtained from Fig. 1 are listed in Table 2. The data exhibited that, the corrosion current density (I_{corr}) decreases, and the inhibition efficiency ($\eta\%$) increases as the concentration of inhibitors is increased. These results suggest that retardation of the electrodes processes occurs, at both cathodic and anodic sites, as a result of coverage of these sites by surfactants molecules. However, the maximum decrease in I_{corr} was observed for inhibitor **II**. The increase of inhibitor efficiency with increasing the concentration can be interpreted on the basis of the adsorption amount and the coverage of surfactants molecules, increases with increasing concentration [20,21]. The E_{corr} values of all synthesized inhibitors were shifted slightly toward both cathodic and anodic directions and did not show any definite trend in CO_2-saturated 1% NaCl solution. This may be considered due to the mixed-type behavior of the studied inhibitors. It can be observed that, the shift in E_{corr} is characteristic of anodic and anodic/cathodic inhibitor [22]. Moreover, the increases in the cathodic and anodic

Table 2 Corrosion parameters obtained from Tafel polarization for mild steel in CO_2-saturated 1% NaCl solution in the absence and presence of different concentrations of the prepared surfactants at 50 °C.

Inhibitors code	Conc. of inhibitor (ppm)	I_{corr} ($\mu A\ cm^{-2}$)	$-E_{corr}$ (mV (Ag/AgCl))	β_a (mV dec^{-1})	$-\beta_c$ (mV dec^{-1})	θ	$\eta\%$
Absence	**0.0**	**389**	**687**	**44**	**107**	–	–
I	25	89.50	689	47	110	0.769	76.99
	50	72.85	685	49	116	0.812	81.27
	75	61.50	682	54	121	0.841	84.19
	100	21.78	693	61	125	0.944	94.40
II	25	54.73	682	50	108	0.859	85.93
	50	40.45	677	57	11	0.896	89.60
	75	21.16	695	62	119	0.945	94.56
	100	4.66	699	69	129	0.988	98.80

Tafel slopes (β_c and β_a) are related to the decrease in both the cathodic and anodic currents. This indicates that natural naphthenate surfactants powerfully inhibit the corrosion process of the mild steel in the investigated media, and its ability as a corrosion inhibitor is enhanced as its concentration. Conclusively, the surfactant inhibitor, having near unity θ (Table 2), was considered as a good physical barrier shielding the corroding surface from corrosive medium and dumping the corrosion rate of mild steel significantly.

Addition of natural naphthenates surfactants to the chloride solutions saturated with CO_2 decreases the currents' density significantly and the increase in its concentration is shown to increase the effect. This provides another confirmation of the ability of surfactant molecule to be adsorbed by forming a protective layer on the steel surface and to prevent it from corrosion.

3.3. Linear polarization resistance (LPR) corrosion rate

LPR test has been performed in brine saturated with CO_2 at 50 °C, in turbulence fluid stream during 20 h. Fig. 2 shows that, the change in corrosion rate (CR) with time for mild steel in CO_2-saturated 1%NaCl solution containing different concentrations from inhibitors (a) I and (b) II at 50 °C. The inhibitor was added after 1 h of exposure because at this time the corrosion potential got stable, allowing the measurement of the CR prior the injection of the inhibitor. The initial corrosion rate, without inhibitor, was measured to be between 3.45 and 5.03 mm y^{-1}. It can be observed from Fig. 2 that, the CR, in the absence of inhibitor, tends to increase with time. The increase in CR has been attributed to the galvanic effect between the ferrite phase and cementite (Fe_3C) which is a part of the original steel in the non-oxidized state and accumulates on the surface after the preferential dissolution of ferrite (α-Fe) into Fe^{2+} [23]. Depending on the microstructural properties of the steel, the morphology of these carbides will be different (laminar, globular, etc.) influencing the behavior of the material in a corrosive media. Because the carbide phase could reinforce a protective layer and anchor it to the steel substrate, the size and distribution of these carbides become very important. Therefore, there is a preferential dissolution of ferrite over cementite, the former working as the anode and latter as the cathode, favoring the hydrogen evolved reaction (HER) during the corrosion process [24,25].

Variations in the corrosion rate for inhibitors I and II at different concentrations are presented in Fig. 2. Corrosion parameters were calculated on the basis of LPR corrosion rate test. The inhibition efficiency ($\eta\%$) was calculated according to the following equations [14]:

$$\eta\% = \frac{CR_0 - CR_i}{CR_0} \times 100 \qquad (2)$$

where CR_o is the corrosion rate without inhibitor and CR_i is the corrosion rate when inhibitor is present. It can be seen that the presence of inhibitors results a high decrease in the corrosion rate. In the case of these inhibitors, the corrosion rate decreases as the inhibitor concentration increases, getting maximum inhibition efficiency 95.27 and 99.76% at 100 ppm after 20 h of exposure for inhibitors I and II, respectively. This trend may result from the fact that adsorption and surface coverage increase with the increasing of concentration; thus the surface is effectively separated from the medium [16,17].

Fig. 3 shows the calculated values of corrosion rates and the inhibition efficiencies in the absence and presence of different concentrations of different inhibitors at 50 °C. The data exhibited that, the corrosion rates and the inhibition efficiencies are found to depend on the concentration of the inhibitors. The corrosion rate (CR) are decreased, and the inhibition efficiencies ($\eta\%$) are increased with the increase of the surfactant concentrations. This could be explained on the basis of inhibitor adsorption on the metal surface and the adsorption process enhances with increasing inhibitor concentration, forming a barrier film which prevents the aggressive medium from attacking the metal surface. Adsorption can occur either directly on the basis of donor–acceptor interaction between the unshared electron pairs and/or π-electrons of inhibitor molecule and the vacant d-orbitals of the metal surface atoms or by interaction of the inhibitors with already adsorbed chloride ions [26].

The high inhibition efficiency obtained in CO_2-saturated 1% NaCl solution in the presence of studied surfactants can be attributed to the formation of a protective film of iron carbonate ($FeCO_3$) in the metal surface. The properties of the formed layers and its effect on the corrosion rate are important factors to take into account when studying the corrosion of mild steels in CO_2-saturated solutions. Ogundele and White suggested that, iron carbonate, $FeCO_3$, may be important in the formation of protective layers on steel surface [27]. The formation of iron carbonate can be explained using the following equations [14]:
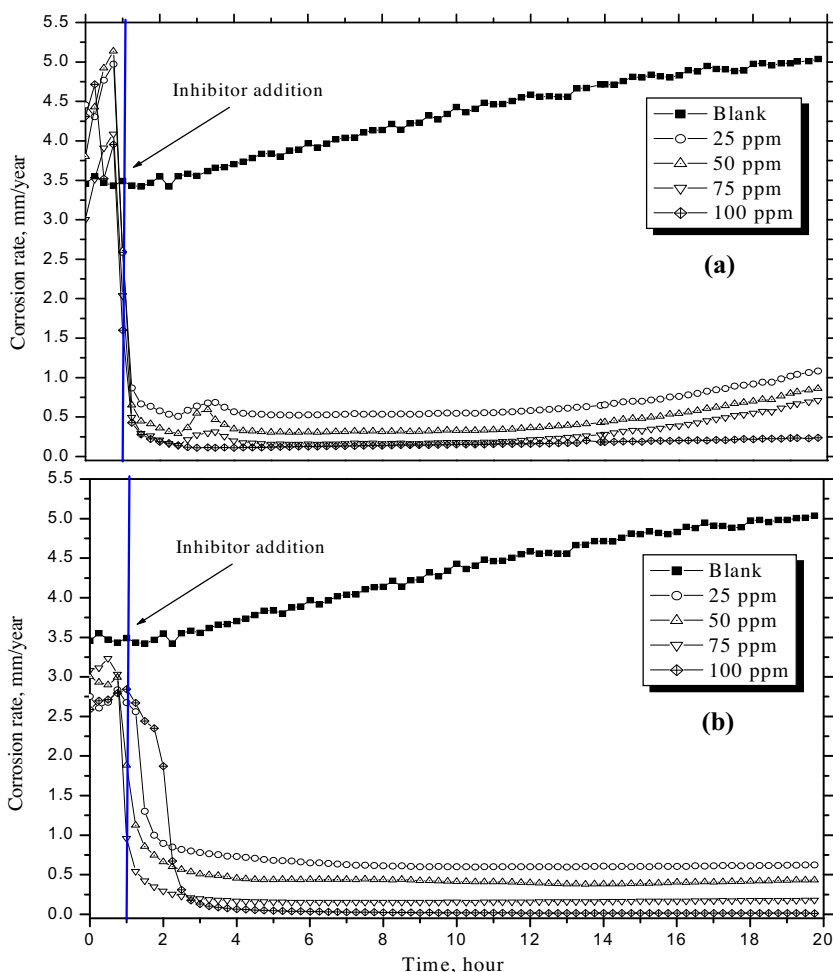
$$Fe^{2+} + CO_3^{2-} \rightarrow FeCO_3 \qquad (3)$$

Figure 2 Variation of the Corrosion rate with time for mild steel in CO_2-saturated 1% NaCl solution containing different concentrations of inhibitors (a) **I** and (b) **II** at 50 °C.
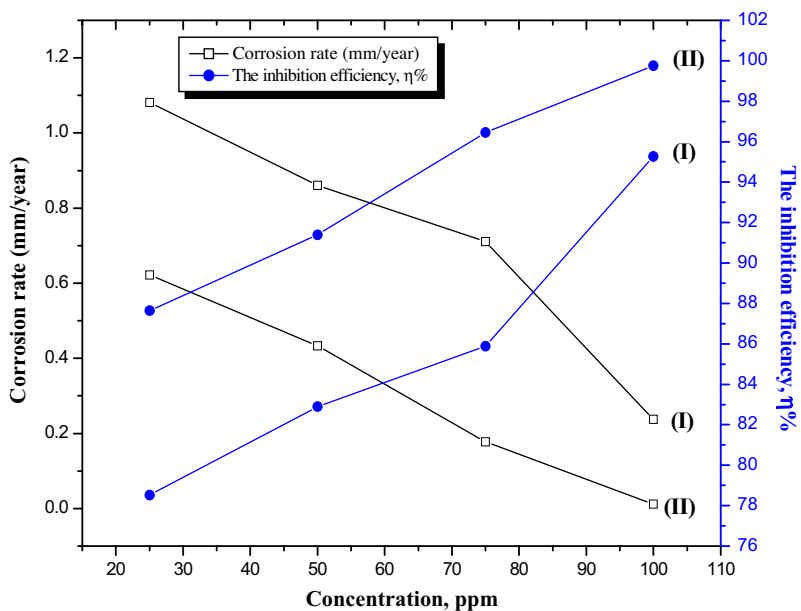

Figure 3 Dependence of inhibition efficiency and corrosion rate of mild steel on the concentration of inhibitors in CO_2-saturated brine at 50 °C.
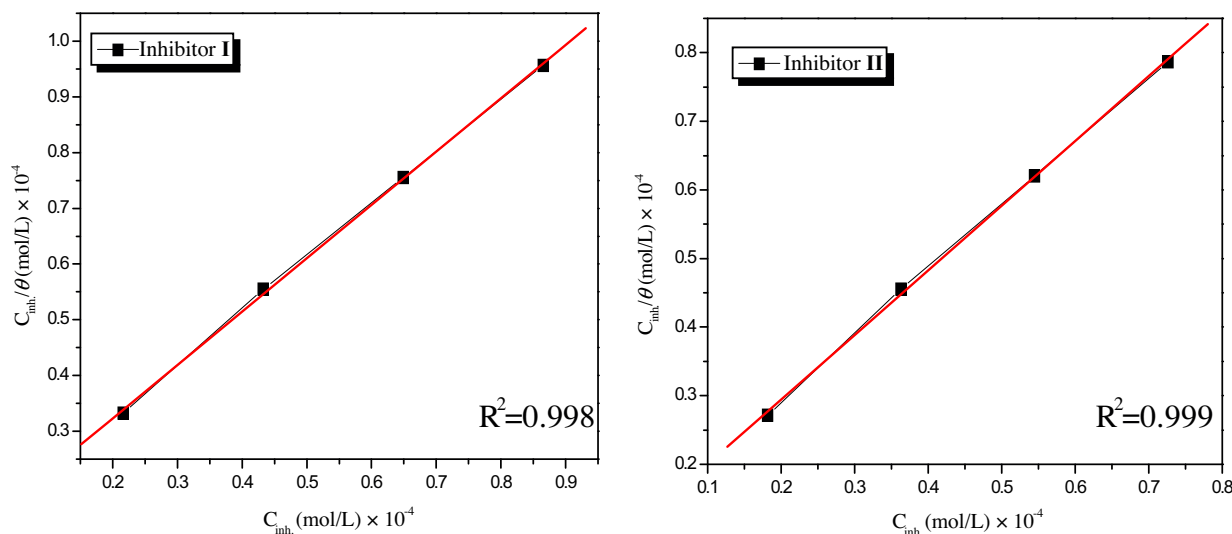
Figure 4   Langmuir plots for inhibitors **I** and **II** in CO_2-saturated brine obtained from polarization measurements at 50 °C.

By comparison between inhibition efficiency values ($\eta\%$) which are calculated from both LPR corrosion rate and extrapolation of anodic and cathodic curves, we find that both have a similar trend. In other words, the inhibition efficiency increases with increasing surfactant concentration, and the maximum inhibition efficiency values are obtained at 100 ppm in the case of all investigated inhibitors. It is noteworthy that, the values of inhibition efficiency obtained by LPR corrosion rate results are greater than those obtained by cathodic and anodic extrapolation curves. Such results can be attributed to the different interactions of surfactant molecule with the metal surface during cathodic and anodic polarization.

It is clear that the $\eta\%$ values increased and that the CR values decreased with increasing inhibitor concentration. This result indicates a decrease in the active surface area caused by the adsorption of the inhibitors on the mild steel surface, and it suggests that the corrosion process became hindered; this hypothesis is corroborated by the anodic and cathodic polarization curves and the corrosion potential results. The best result for the inhibition efficiency of inhibitors was obtained with the diethylamine complex, with efficiency equal to 97.76% at a concentration of 100 ppm. We did not perform the analyses with high concentrations for the surfactant because at 100 ppm, this inhibitor already produced a good result for inhibition efficiency. The efficiency of the dimethylamine complex was 95.27% at the same concentration.

3.4. Adsorption isotherm

The surface coverage, θ, was calculated using the following equation [28]:

$$\theta = \frac{I_{uninh.} - I_{inh.}}{I_{uninh.}} \tag{4}$$

The values of the degree of surface coverage (θ) obtained from polarization measurements for the tested inhibitors have been applied to different adsorption isotherms. Since adsorption isotherms can provide important clues to the nature of metal–inhibitor interaction it was established that isotherms describe the adsorptive behavior of the studied corrosion inhibitors. The best correlation among the experimental results

was found to fit the Langmuir adsorption isotherm as shown in Fig. 4. Plotting C_{inh}/θ versus C_{inh} yielded a straight line with a correlation coefficient (R^2) higher than 0.998 and a slope closed to 1 according to the following equation [29]:

$$\frac{C_i}{\theta} = \frac{1}{K_{ads.}} + C_i \tag{5}$$

where C_{inh} is the inhibitor concentration and K_{ads} is the adsorption equilibrium constant of the inhibitor on mild steel surface.

This indicates that the adsorption of these surfactants can be fitted to a Langmuir adsorption isotherm. The strong correlation of the Langmuir adsorption isotherm may confirm the validity of this approach. The equilibrium constant (K_{ads}) for the adsorption–desorption process of these compounds can be calculated from reciprocal of the intercept. The adsorptive equilibrium constant (K_{ads}) values are 11.8×10^5 and 13.5×10^5 M^{-1} for inhibitors **I** and **II**, respectively. It is clear that, the large values indicate a strong adsorption of the synthesized surfactants on the surface of mild steel in CO_2-saturated 1% NaCl solution. This may be due to the formation of coordinated bonds between the unshared electron pairs and/or π-electrons of inhibitor molecule and the d-orbital of iron on the surface of steel.

The interaction between the inhibitors and mild steel surface can be described by the adsorption isotherm. During corrosion inhibition of metals, the nature of the inhibitor on the corroding surface has been deduced in terms of adsorption characteristics of the inhibitor. Furthermore, the solvent (H_2O) molecules could also be adsorbed at metal/solution interface. So the adsorption of surfactants molecules from aqueous solution can be regarded as a quasi-substitution process between the organic compounds in the aqueous phase [Surfactant$_{(sol.)}$] and water molecules at the electrode surface [$H_2O_{(ads.)}$]:

$$\text{Surfactant}_{(sol.)} + x\text{H}_2\text{O}_{(ads.)} = \text{Surfactant}_{(ads.)} + x\text{H}_2\text{O}_{(sol.)} \tag{6}$$
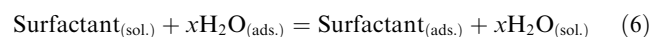
where, x is the size ratio, that is, the number of water molecules replaced by one organic inhibitor. The free energy of adsorption (ΔG_{ads}^o) of the inhibitor on mild steel surface was calculated as follows [30]:
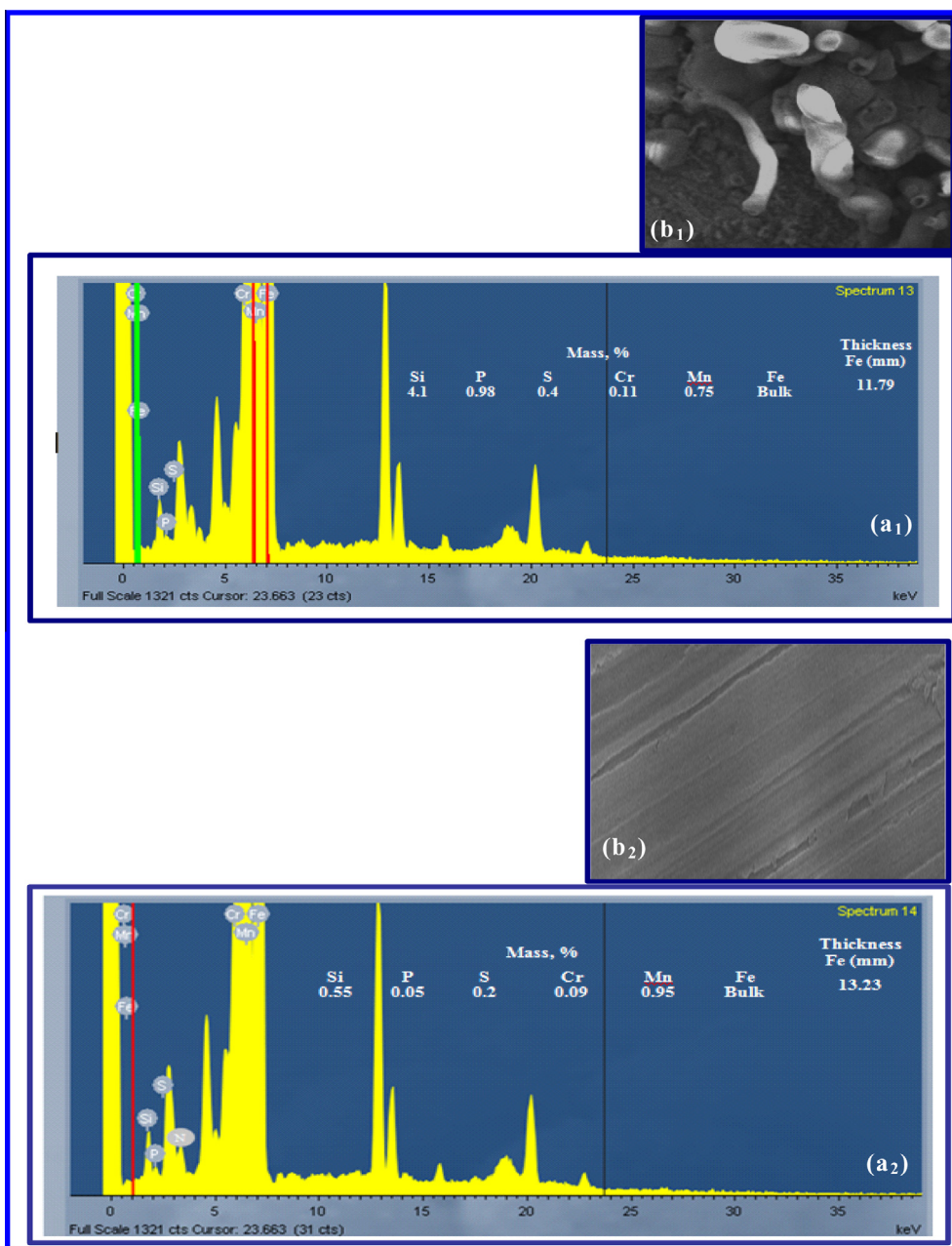
Figure 5 EDRF analysis of mild steel electrode surface after immersion in CO_2-saturated 1% NaCl for 3 days: (a_1) without inhibitor; (a_2) in the presence of 100 ppm inhibitor **II**; SEM of mild steel electrode surface after immersion in CO_2-saturated 1% NaCl for 3 days: (b_1) without inhibitor and (b_2) in the presence of 100 ppm inhibitor **II**.

$$\Delta G_{ads} = -2.303 RT \ \log(55.5 \ K_{ads}) \qquad (7)$$

The values of ΔG_{ads}^o are -48.3 and -48.7 kJ mol^{-1} for inhibitors **I** and **II**, respectively. The negative values of ΔG_{ads}^o indicate the spontaneous adsorption of the prepared inhibitors on mild steel surface [29]. Generally, values of ΔG_{ads}^o up to -20 kJ mol^{-1} are consistent with the electrostatic interaction between the charged molecules and the charged metal (physical adsorption) while those more negative than -40 kJ mol^{-1} involve sharing or transfer of electrons from the inhibitor molecules to the metal surface to form a coordinate type of bond (chemisorption) [31]. The obtained values of the adsorption free energy, ΔG_{ads}^o, were found to be more than -40 kJ mol^{-1} are indicative of chemisorption [32–34].

3.5. Surface analysis

In order to see if the surfactant molecules are indeed adsorbed on the mild steel surface we carried out the EDRF with a microscope system analyses. Fig. 5a$_1$ shows an EDRF spectroscopy for mild steel surface in the investigated solution without inhibitors, exhibits the characteristics peaks related to Fe, Mn, P, Cr and oxygen elements. This indicated that the corrosion product on mild steel surface being metal oxide. However, the data in Fig. 5a$_2$ in the presence of 100 ppm of inhibitor **II** show additional peaks characteristic of N element. This result proved that the adsorption of inhibitor molecule on mild steel surface leads to a decrease of the corrosion layer,

and higher concentration of the inhibitor is necessary to delay the corrosion process.

From quantitative analysis it can be observed that, the mass thickness of iron for the electrode surface is 12.75 mm. In the aggressive media without inhibitors, there is a decrease in the mass thickness of iron on the electrode surface after corrosion process (11.79 mm), but in the presence of 100 ppm of inhibitor **II**, the mass thickness increased to 13.23 (Fig. 5a$_1$ and a$_2$). The quantitative analysis showed that, the presence of inhibitor in CO_2-saturated brine an adsorbed layer is formed on the electrode surface, which successfully inhibits corrosion processes.

Fig. 5b$_1$ shows a SEM photograph recorded for mild steel surface after immersion in CO_2-saturated 1% NaCl solutions for 3 days in the absence of inhibitors, the results exhibited that thick porous layer of corrosion product covered all electrode surfaces, disclosing that in free corrosive solution, the surface is highly corroded. In case of mild steel immersed in CO_2-saturated 1% NaCl solutions in the presence of 100 ppm of inhibitor **II** (NDEC) at the same conditions, a smooth surface was noticed (Fig. 5b$_2$), which indicates a good protective film present on the mild steel surface. The analysis obtained from EDRF-SEM is agreed with the results obtained in our electrochemical measurements, which suggests that the metal surface was protected through the adsorption of inhibitor molecule on its surface, thereby reducing the metal dissolution.

4. Conclusions

LPR corrosion rate and Tafel polarization methods are used to study corrosion of mild steel in CO_2-saturated 1% NaCl solution and the inhibiting effect of two natural naphthenates surfactants. LPR corrosion rate measured within 20 h shows that all studied compounds act as inhibitors in the investigated medium. The highest inhibition efficiency is obtained by compound **II** (99.76% at 100 ppm).

Analysis of the polarization data show that the inhibiting properties increase with inhibitor concentration. The inhibition efficiency of inhibitor **II** was found to be more than those of inhibitor **I** for all concentrations. Polarization curves indicate that, the two investigated surfactants are mixed inhibitors.

It is found that the inhibition occurs through adsorption, which obeys the Langmuir adsorption isotherm. Calculated Gibbs free energy of adsorption confirms the chemical nature of the adsorption.

EDRF observations of the electrode surface showed that a good protective film present on the metal surface and also confirms the highest inhibition efficiency of the prepared naphthenates surfactants.

References

[1] S. Ikeda, M. Mukai, Ueda, NACE Corrosion/84, Houston, Texas (1984) Paper No. 289.
[2] X. Jiang, Y.G. Zheng, D.R. Qu, W. Ke, Corr. Sci. 48 (2006) 3091.
[3] G. Zhang, C. Chen, M. Lu, C. Chai, Y. Wu, Mater. Chem. Phys. 105 (2007) 331.
[4] F. Farelas, M. Galicia, B. Brown, S. Nesic, H. Castaneda, Corros. Sci. 52 (2010) 509.
[5] E.W.J. van Hunnik, B.F.M. Pots, E.L.J.A. Hendriksen, NACE Corrosion/96, Houston, Texas (1996) Paper No. 6.
[6] O. Benali, L. Larabi, B. Tabti, Y. Harek, Anti-Corros Method Mater. 52 (2005) 280.
[7] E. Machnikova, Kenton H. Whitmire, N. Hackerman, Electrochim. Acta 53 (2008) 6024–6032.
[8] J.M. Bastidas, P. Pinilla, J.L. Polo, S. Miguel, Corros. Sci. 45 (2003) 427–449.
[9] A.E. Bolzán, I.B. Wakenge, R.C.V. Piatti, R.C. Salvarezza, A.J. Arvia, J. Electroanal. Chem. 501 (2001) 241–252.
[10] E. Stipnisek-Lisac, A. Gazivoda, M. Madzarac, Electrochim. Acta 47 (2002) 4189–4194.
[11] M. Sahin, S. Bilgic, H. Yilmaz, Appl. Surf. Sci. 195 (2002) 1–7.
[12] H. Luo, Y.C. Guan, K.N. Han, Corrosion 54 (1998) 619–627.
[13] C.A. Miller, S. Qutubuddin, in: H.F. Eick, C.D. Parfitt (Eds.), Interfacial Phenomena in Apolar Media, Surfactant Science Series, vol. 21, Markel Dekker Inc., New York, Basel, 1987, p. 166.
[14] Hany M. Abd El-Lateef, V.M. Abbasov, L.I. Aliyeva, T.I. Ismayilov, E.E. Qasimov, T.U. Ahmadov, Global J. Phys. Chem. 3 (14) (2012) 1–12.
[15] Hany M. Abd El-Lateef, V.M. Abbasov, L.I. Aliyeva, E.E. Qasimov, I.T. Ismayilov, J. Surf. Interfaces Mater. 1 (2012) 1–11.
[16] V.M. Abbasov, Hany M. Abd El-Lateef, L.I. Aliyeva, I.T. Ismayilov, E.E. Qasimov, J. Korean Chem. Soc. 57 (2013) 25–34.
[17] V.M. Abbasov, Hany M. Abd El-Lateef, L.I. Aliyeva, I.T. Ismayilov, Application of Some Surfactants Based On Corn Oil as Corrosion Inhibitors for Carbon Steel in CO_2 Environments// NACE corrosion 2013, Florida, USA, Paper No. 2129, pp.1–10.
[18] A.M. Samedov, L.I. Alieva, V.M. Abbasov, Prot. Met. 44 (2008) 397–401.
[19] A. El-Sayed, A.M. Shaker, H.M. Abd El-Lateef, Corros. Sci. 52 (2010) 72.
[20] E. Akbarzadeh, M.N.M. Ibrahim, A.A. Rahim, Int. J. Electrochem. Sci. 6 (2011) 5396–5416.
[21] A. El-Sayed, Hossnia S. Mohran, H.M. Abd El-Lateef, Corros. Sci. 52 (2010) 1976–1984.
[22] D.A. López, S.N. Simison, S.R. de Sánchez, Corros. Sci. 47 (2005) 735–775.
[23] N. Staicopolus, J. Electrochem. Soc. 110 (1963) 1121–1124.
[24] J. Crolet, N. Thevenot, S. Nesic, Corrosion 54 (1998) 194–203.
[25] K. Videm, J. Kvarekvaal, T. Perez, G. Fitzsimons, NACE Corrosion/96, Houston, Texas, 1996, Paper No. 1.
[26] Z. Zhang, S. Chen, Y. Li, S. Li, L. Wang, Corros. Sci. 51 (2009) 291.
[27] G.I. Ogundele, W.E. White, Corrosion 42 (2) (1986) 71.
[28] M.A. Hegazy, M.F. Zaky, Corros. Sci. 52 (2010) 1333–1341.
[29] S.A. Abd, A.S. El-Maksoud, Fouda, Mater. Chem. Phys. 93 (2005) 84–90.
[30] A.M. Badawi, M.A. Hegazy, A.A. El-Sawy, H.M. Ahmed, W.M. Kamel, Mater. Chem. Phys. 124 (2010) 458–465.
[31] M. Abdallah, Corros. Sci. 44 (2002) 717–728.
[32] Z. Szklarska-Smialowska, Corros. Sci. 18 (1978) 97–101.
[33] Hany M. Abd El-Lateef, V.M. Abbasov, L.I. Aliyeva, E.E. Qasimov, I.T. Ismayilov, Mater. Chem. Phys. 142 (2013) 502–512.
[34] V.M. Abbasov, Hany M. Abd El-Lateef, L.I. Aliyeva, E.E. Qasimov, I.T. Ismayilov, Mai M. Khalaf, Egypt. J. Pet. 22 (2013) 451–470.